Effects of dietary phosphate on glucose and lipid metabolism

Maerjianghan Abuduli,[1] Hirokazu Ohminami,[1] Tamaki Otani,[2] Hitoshi Kubo,[3] Haruka Ueda,[1] Yoshichika Kawai,[4] Masashi Masuda,[1] Hisami Yamanaka-Okumura,[1] Hiroshi Sakaue,[5] Hironori Yamamoto,[6] Eiji Takeda,[1] and Yutaka Taketani[1]

[1]*Department of Clinical Nutrition and Food management, Institute of Biomedical Sciences, Tokushima University Graduate School, Tokushima, Japan;* [2]*Radioisotope Research Center, Tokushima University Graduate School, Tokushima, Japan;* [3]*Advanced Clinical Research Center, Fukushima Medical University, Fukushima City, Japan;* [4]*Department of Food Science, Institute of Biomedical Sciences, Tokushima University Graduate School, Tokushima, Japan;* [5]*Department of Nutrition and Metabolism, Institute of Biomedical Sciences, Tokushima University Graduate School, Tokushima, Japan; and* [6]*Department of Health and Nutrition, Faculty of Human Life, Jin-ai University, Echizen, Japan*

Abuduli M, Ohminami H, Otani T, Kubo H, Ueda H, Kawai Y, Masuda M, Yamanaka-Okumura H, Sakaue H, Yamamoto H, Takeda E, Taketani Y. Effects of dietary phosphate on glucose and lipid metabolism. *Am J Physiol Endocrinol Metab* 310: E526–E538, 2016. First published January 19, 2016; doi:10.1152/ajpendo.00234.2015.— Recent epidemiological and animal studies have suggested that excess intake of phosphate (P_i) is a risk factor for the progression of chronic kidney disease and its cardiovascular complications. However, little is known about the impact of dietary high P_i intake on the development of metabolic disorders such as obesity and type 2 diabetes. In this study, we investigated the effects of dietary P_i on glucose and lipid metabolism in healthy rats. Male 8-wk-old Sprague-Dawley rats were divided into three groups and given experimental diets containing varying amounts of P_i, i.e., 0.2 [low P_i (LP)], 0.6 [control P_i (CP)], and 1.2% [high P_i (HP)]. After 4 wk, the HP group showed lower visceral fat accumulation compared with other groups, accompanied by a low respiratory exchange ratio ($\dot{V}_{CO_2}/\dot{V}_{O_2}$) without alteration of locomotive activity. The HP group had lower levels of plasma insulin and nonesterified fatty acids. In addition, the HP group also showed suppressed expression of hepatic lipogenic genes, including sterol regulatory element-binding protein-1c, fatty acid synthase, and acetyl-CoA carboxylase, whereas there was no difference in hepatic fat oxidation among the groups. On the other hand, uncoupling protein (UCP) 1 and peroxisome proliferator-activated receptor-γ coactivator-1α (PGC-1α) expression were significantly increased in the brown adipose tissue (BAT) of the HP group. Our data demonstrated that a high-P_i diet can negatively regulate lipid synthesis in the liver and increase mRNA expression related to lipid oxidation and UCP1 in BAT, thereby preventing visceral fat accumulation. Thus, dietary P_i is a novel metabolic regulator.

dietary phosphate; energy metabolism; brown adipose tissue; visceral fat

OBESITY CONTINUES TO BE A MAJOR PUBLIC HEALTH PROBLEM worldwide. Overnutrition and an increased consumption of fast foods are primary factors contributing to this problem. Fast foods or processed foods have high energy density and also frequently contain a large amount of P_i as a food additive. Recent epidemiological studies have suggested that a high dietary P_i intake can be associated with increased cardiovascular risk and other metabolic disorders.

P_i is an essential nutrient that significantly affects skeletal formation, energy metabolism, and intracellular signaling (43, 45). P_i homeostasis is regulated by the absorption of P_i in the intestine, bone formation/resorption, and reabsorption of P_i in the kidney. The kidney is particularly important in the regulation of P_i homeostasis (36, 45). Most P_i-regulating factors, such as high/low P_i intake, 1,25-dihydroxyvitamin D [$1,25(OH)_2D$], parathyroid hormone (PTH), and fibroblast growth factor 23 (FGF23), can regulate P_i reabsorption in the kidney to maintain the P_i homeostasis (6, 36, 43).

Recent epidemiological and animal studies have suggested that an excessive intake of P_i is a risk factor for the progression of chronic kidney disease and the occurrence of cardiovascular complications (8, 45). Excess P_i has been independently associated with cardiovascular morbidity and mortality (1, 7). On the other hand, metabolic syndrome represents an important cluster of risk factors for the development of cardiovascular disease (32, 48), and it was proposed recently that disturbances in P_i metabolism may be a key feature of metabolic syndrome, since both too high and too low serum P_i levels have been correlated with cardiovascular risk factors and elements of metabolic syndrome (19, 23, 40). It may be important to maintain an appropriate serum level of P_i for the prevention of cardiac disease and metabolic syndrome. In addition, Ellam et al. (14) also demonstrated that a high-P_i diet accelerated atherogenesis in apolipoprotein E knockout mice, whereas low dietary P_i intake induced insulin resistance, adiposity, and hepatic steatosis. Our recent studies have also shown that dietary P_i restriction induces hepatic lipid accumulation through dysregulation of cholesterol metabolism in mice (46). However, the mechanisms by which an excessive amount of dietary P_i could influence glucose and lipid metabolism have not been clarified. Thus, the aim of this study was to investigate the effects of dietary P_i on glucose and lipid metabolism in healthy rats. We demonstrated that high P_i intake suppressed body weight gain as a result of decreased hepatic lipogenesis and increased fat oxidation and UCP1 in BAT, which is indicative of augmented BAT activation.

MATERIALS AND METHODS

Animals and diets. Seven-week-old male Sprague-Dawley (SD) rats were purchased from SLC (Shizuoka, Japan) and were housed in individual cages in an animal room maintained under standard conditions with 12 h light-dark cycle and temperature (22 ± 22°C) and provided with ultrapure water. Animals were divided into three experimental groups based on body weight and fed either 0.2 [low P_i (LP)], 0.6 control P_i (CP), or 1.2% [high P_i (HP)] P_i diet, respectively, by a pair-feeding procedure for 4 or 14 wk. The composition of each

Table 1. *Composition of experimental diets*

	LP	CP	HP
P_i dose	0.2%	0.6%	1.2%
Ca dose	0.6%	0.6%	0.6%
AIN-93G	59.5	59.5	59.5
Milk casein	20	20	20
Sugar	5.27	5.27	5.27
Mineral mix	1.56	1.56	1.56
$CaCO_3$	1.5	1.5	1.5
KH_2PO_4	0.77	2.53	5.17
Soybean oil	7	7	7
Dextrin	4.39	2.64	0
Total	100	100	100

LP, low-phosphate diet; CP, control phosphate diet; HP, high-phosphate diet. We used a mineral mix and an altered AIN-93G diet derived from casein, $CaCO_2$, and KH_2PO_4.

diet is shown in Table 1. The body weights of the rats were checked weekly during the experimental period, and their amount of daily food intake was recorded.

All rats were fasted overnight (12–14 h) prior to euthanization under anesthesia. Blood was collected into tubes containing heparin, and then plasma was separated by centrifugation at 2,000 g for 4 min and stored at $-30°C$ until further analysis. The liver, kidney, muscle, brown adipose tissue, and epididymal fat samples were washed in 0.9% NaCl and immediately snap-frozen in liquid nitrogen and stored at $-80°C$. All animal studies were carried out in accordance with established guidelines for the care and handling of laboratory animals and were approved by the Animal Care and Use Committee of Tokushima University.

Oral glucose tolerance test. Oral glucose tolerance tests were performed after 3 wk of dietary intervention. The rats were fasted for 12 h before testing. Subsequently, a standard dose of glucose (2 g/kg body wt) was administered via gavage, and blood glucose levels were determined with a glucometer (Accu-Check) at 0, 15, 30, 60, 90, and 120 min after gavage in blood from the tail vein. Serum insulin levels were determined by an ultrasensitive rat enzyme kit (Morinaga). The homeostasis model assessment of insulin resistance (HOMA-IR) scores were calculated using fasting glucose and fasting insulin concentrations obtained from rats after 12–14 h of fasting and using the following formula: fasting blood glucose (mg/dl) $\times$ fasting insulin (ng/ml)/405.

O_2 consumption, respiratory quotient, and locomotive activity. O_2 consumption and CO_2 production were measured continuously over 3 days using an Oxymax apparatus (Columbus Instruments, Columbus, OH). Animals were housed individually in sealed chambers with free access to food and drinking water. Each cage was monitored for both

O_2 consumption and CO_2 production at 10-min intervals. Oxygen consumption and CO_2 were expressed as liters of O_2 or $CO_2 \cdot kg$ body $wt^{-1} \cdot h^{-1}$. Locomotive activity was measured by using an infrared-based locomotive activity measurement device (ACTIMO; Bioresearch Center, Tokyo, Japan).

Real-time PCR. Total RNA was isolated from 100 mg of liver tissue using RNAiso Plus reagent (Takara). The brown part of the interscapular fat or epididymal fat was dissected. Total RNA was isolated from brown adipose tissue and epididymal fat using an RNeasy lipid tissue mini kit (Qiagen) according to the manufacturer's instructions. The cDNA was synthesized from 2.5 μg of RNA using a reverse transcriptase kit (Invitrogen, Carlsbad, CA) with an oligo-dT primer. After cDNA synthesis, quantitative real-time PCR was performed in 20 μl of SYBR Green PCR master mix using a real time PCR system (Applied Biosystems, Carlsbad, CA). The amplification programs were set as follows: initial denaturation at 95°C for 10 min, followed by 50 cycles of 95°C for 10 s, 60°C for 15 s, and 72°C for 15 s. The PCR products were checked by melting-curve analysis and 2% agarose gel electrophoresis. All sample mRNA levels were normalized to values for β-actin mRNA amplification, and the relative levels of gene expression were calculated by using the comparative C_T method. The primer sequences used for real-time PCR analysis are shown in Table 2.

Hepatic lipid contents. Hepatic lipids were extracted from 1.0 g of liver with chloroform-methanol (2:1, vol/vol), according to the method of Folch et al. (17). Hepatic triglyceride (TG) and total cholesterol (T-Cho) concentrations were analyzed using the same protocol as that described for plasma triglyceride analysis. The TG and T-Cho contents were normalized by tissue weight.

Histology. The brown part of the interscapular fat was dissected and rinsed in phosphate-buffered saline (PBS) and then fixed in 4% buffered formalin. After an overnight wash, specimens were dehydrated in graded ethanol, cleared in xylene, and paraffin embedded, preserving their anatomic orientation. Sections (4–5 μm in thickness) were cut from paraffin blocks using a microtome, mounted on polylysine-coated slides, and stored at room temperature. For histochemical analysis, 2- to 5-μm-thick paraffin sections were cut, deparaffinized, and stained with haematoxylin-eosin.

Biochemical analysis. Plasma P_i, calcium, creatinine, and blood urea nitrogen (BUN) levels were measured using phospha-C, calcium-E, creatinine, and BUN test kits (Wako, Osaka, Japan), respectively. The concentration of PTH in plasma was measured by a Rat Intact PTH ELISA kit (Immutopics, San Clemente, CA), and plasma FGF23 was measured by an FGF23 ELISA kit (Kainos Laboratories, Tokyo, Japan). The concentration of leptin in plasma was determined using an ELISA kit (Morinaga), and that of adiponectin was determined using an ELISA kit (R & D Systems). The plasma $1,25(OH)_2D$ concentration was analyzed by SRL (Tachikawa). The T-cho, TG, and

Table 2. *Sequence of oligonucleotide primers of quantitative RT-PCR analysis*

Gene Name	Forward	Reverse
ACC	5′-CCAGTCTACATCCGCTTGGCTGAG-3′	5′-AGTCGCCAGTAGAAGAAGGTGCGG-3′
FAS	5′-TGGGCCCAGCTTCTTAGCC-3′	5′-GGAACAGCGCAGTACCGTAGA-3′
SREBP-1c	5′-GGAGCCATGGGATTGCACATTT-3′	5′-TCCTTCCGAAGGTCTCTCCTC-3′
PGC-1α	5′-TGTTCGATGTGTCGCCTTCT-3′	5′-GAACGAGAGCGCATCCTTTG-3′
CPT-1	5′-GGTGGGCCACAAATTACGTG-3′	5′-CAGCATCTCCATGGCGTAGT-3′
UCP1	5′-ACAGAAGGATTGCCGAAACT-3′	5′-GATCTTGCTTCCCAAAGAGG-3′
UCP2	5′-TCTCCCAATGTTGCCCGAAA-3′	5′-GGGAGGTCGTCTGTCATGAG-3′
HSL	5′-AGAGCCATCAGACAGCCCCGAGAT-3′	5′-TGACGAGTAGAGGGGCATGTGGAG-3′
ChREBP	5′-CAGCTTCTCGACTTGGACTG-3′	5′-TTGCCAACATAAGCGTCTTC-3′
ACO	5′-ATGGCAGTCCGGGAGAATACCC-3′	5′-CCTCATAACGGCTGGCTTCGAGT-3′
PPARα	5′-TGTATGAAGCCATCTTCACG-3′	5′-GGCATTGAACTTCATAGCGA-3′
β-Actin	5′-GTCCCAGTATGCCTCTGGTCGTAC-3′	5′-CCACGCTCGGTCAGGATCTTCATG-3′

ACC, acetyl-CoA carboxylase; FAS, fatty acid synthase; SREBP-1c, sterol regulatory element-binding protein-1c; PGC-1α, peroxisome proliferator-activated receptor (PPAR)-γ coactivator-1α; CPT-1, carnitine palmitoyltransferase 1; UCP1 and -2, uncoupling protein 1 and 2, respectively; HSL, hormone-sensitive lipase; ChREBP, carbohyrate response element-binding protein; ACO, acyl-CoA oxidase.

nonesterified fatty acids (NEFA) concentrations were determined using specific assay kits (Wako, Osaka, Japan).

PET/CT protocol. Male SD rats aged 8 wk were used in this experiment. The rats were divided into three groups and fed the experimental diets for 4 wk. PET/CT imaging was performed in the P_i diet treatment group before the experimental diet was started as a baseline (pre) and 4 wk after. [^{18}F]fludeoxyglucose ([^{18}F]FDG) PET/CT data were acquired using a Siemens Inveon small-animal PET/CT scanner (Siemens Healthcare, Knoxville, TN). All rats were fasted for 12–15 h, and then body weights and blood glucose levels were measured. Before PET/CT analysis, rats were anaesthetized using inhalant isoflurane (2%) throughout all imaging sessions. The rats were placed in a prone position on the bed of the PET/CT scanner, and a respiration pad was placed under their abdomen. Before the PET scan, rats had a CT scan for attenuation correction and anatomic delineation of PET images. [^{18}F]FDG (average radioactivity 13.0 MBq/rat) was administrated through the tail vein just after the start of PET data acquisition. PET data were acquired for 90 min, and data were reconstructed as $128 \times 128 \times 159$ matrices with a transaxial pixel size of 0.776 mm.

Image analysis. [^{18}F]FDG uptake in the BAT was quantified using the image analysis software Inveon Research Workplace (Siemens Medical Solutions, Malvern, PA). The magnitude of BAT [^{18}F]FDG activation was expressed as a standard uptake value (SUV), which was defined as the average [^{18}F]FDG activity in each volume of interest (VOI) divided by the injected dose (MBq) times the body weight of rats (g) (5). VOIs were selected based on PET images for interscapular BAT and CT images for interscapular white adipose tissue (WAT), similar to previously described methods (42). After the VOIs were visually delineated, Hounsfield unit (HU) levels were thresholded to maximize the difference between BAT and WAT. The kinetic modeling was performed similarly to previously described methods (34). The kinetic rate constants k_1, k_2, and k_3 were estimated. The [^{18}F]FDG rate constants k_1 and k_2 are mediated by glucose transporters across cytomembranes, and k_3 represents phosphorylation by hexokinase (35). The FDG influx constant (k_i) was computed as $k_i = k_1 \times k_3/(k_2 + k_3)$.

Cell culture and differentiation. HB2 cells (kindly provided by Prof. Masayuki Saito) were isolated from BAT of p53 knockout mice and were differentiated into mature brown adipocytes, as described previously (24). In short, HB2 cells were seeded on collagen-coated dish and cultured in high-glucose medium (Sigma-Aldrich, Tokyo, Japan) supplemented with 10% fetal bovine serum (Invitrogen) and 1% penicillin-streptomycin. The medium was changed every 2 days until confluence. Then, 0.5 mM 3-isobutyl-1-methylxanthine and 1 μM dexamethasone were added to induce differentiation. Two days after induction, the medium was changed to differentiation medium with 10 μg/ml insulin and 50 nM triiodothyronine (T_3). For P_i stimulation experiments, we prepared sodium phosphate buffer (0.1 M Na_2HPO_4/NaH_2PO_4, pH 7.4) and added in differentiation medium to produce final P_i concentrations of 0.9, 2, and 3 mM. P_i treatment started on *day 0* of differentiation, as indicated in the figure legends. For PTH [human parathyroid hormone (1–34 fragment), Sigma-Aldrich, Japan] and FGF23 (recombinant human FGF23; R & D Systems), stimulation experiments were also started on *day 0* of differentiation, as described in the figure legends.

Data analysis. Values are expressed as means ± SE. Data were analyzed for differences between groups by Tukey-Kramer post hoc multiple comparisons test of one-way ANOVA. All data analysis was performed using GraphPad Prism 5 software (Graphpad Software, San Diego, CA). $P < 0.05$ was considered to indicate statistical significance.

Fig. 1. Body weight changes and food intake, visceral fat mass, and adipocyte hormones. *A* and *B*: body weight changes (*A*) and food intake (*B*) during dietary intervention. Body weight was measured every day during the experiment, and food intake was measured under the pair-feeding conditions during the light period every other day, and here the weekly average values are presented (*n* = 6 for each group). *C* and *D*: body weight (*C*) and visceral fat mass (*D*) at 4 wk after the experimental diet period was started. Adipose tissues were measured as epididymal (eWAT), mesenteric (mWAT), and retroperitoneal white adipose tissue (rpWAT) depots. *E* and *F*: fasting plasma leptin (*E*) and fasting plasma adiponectin (*F*) levels in rats at 4 wk after the experimental diet period was started. Data are presented as means ± SE (*n* = 6). *$P < 0.05$; **$P < 0.01$. LP, low P_i; CP, control P_i; HP, high P_i.
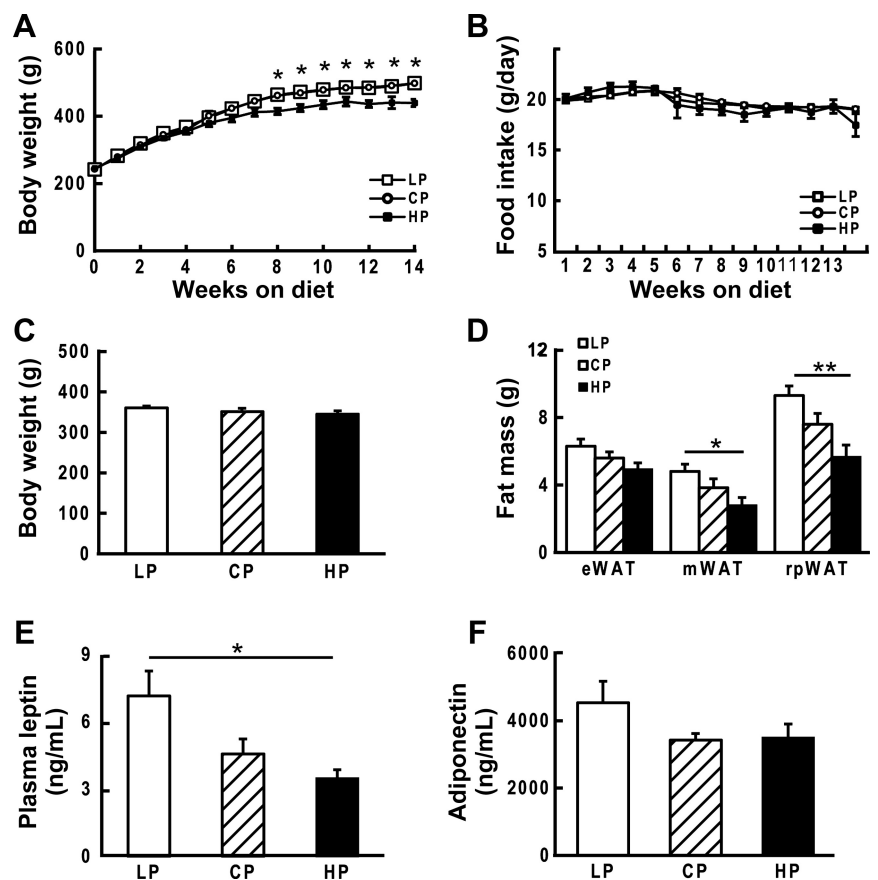
RESULTS

Body weight change and visceral fat mass. Rats fed the HP diet showed significantly attenuated weight gain at 8 wk after the start of feeding (Fig. 1*A*) despite there being no differences in total food intake among the three diet groups throughout the experimental period (Fig. 1*B*). In addition, when the rats were fed with the HP diet for 14 wk, the liver TG content was significantly lowered compared with the LP diet group (LP: 4.22 ± 0.79 mg/g; CP: 2.57 ± 0.51 mg/g; HP: 1.36 ± 0.35 mg/g; $P < 0.05$, LP vs. HP, $n = 4–6$). These data indicate that dietary P_i may affect energy metabolism in rats. To investigate the cause of reduced body weight gain in the HP group, we examined body weight and energy metabolism in that group at 4 wk after the start of feeding. At 4 wk, we did not find any significant differences in body weight (Fig. 1*C*) or the weights of liver, muscle, or other organs among groups (Fig. 2). However, HP group rats exhibited the lowest amount of visceral fat accumulation (Fig. 1*D*). Consistent with the decrease in the fat accumulation, HP group rats showed a marked decrease in their plasma leptin level compared with that of LP group rats (Fig. 1*E*), whereas the plasma adiponectin level showed no significant differences among groups (Fig. 1*F*).

Respiratory quotient and oxygen consumption. To elucidate the cause of the reduced body weight gain in the HP group, we measured the whole body metabolic rate by indirect calorim-etry. Although there were no significant differences in oxygen consumption ($\dot{V}O_2$) or carbon dioxide production ($\dot{V}CO_2$) rates among the three groups (Fig. 3, *A* and *B*), the respiratory quotient (RQ) (Fig. 3*C*), which reflects carbohydrate and fat oxidation, was significantly decreased in the HP group during the dark phases compared with the CP group and was slightly decreased during the light phases (Fig. 3*D*). Plasma free T_3 and free thyroxine 4, which can affect the basal energy expenditure (44), were also not different among the diet groups (Table 3). In addition, we investigated whether locomotive activity in the HP diet group was increased or not. As shown in Fig. 3*E*, there were no significant changes in locomotive activity between the CP and the HP diet groups. Taken together, these results indicate that the decreased body weight of HP group rats was at least in part due to the preferential consumption of fat for energy production.

Plasma marker and lipid profile. There were no significant differences in plasma P_i and calcium levels among the groups (Table 4). However, the plasma level of PTH was significantly higher in the HP group than in the LP and CP groups, and another phosphaturic hormone, FGF23, showed a trend toward being increased in the HP group compared with the LP and CP groups. Urinary P_i excretion in the HP group rats was significantly higher than that of the LP and CP groups. Interestingly, the plasma level of active vitamin D was significantly higher in
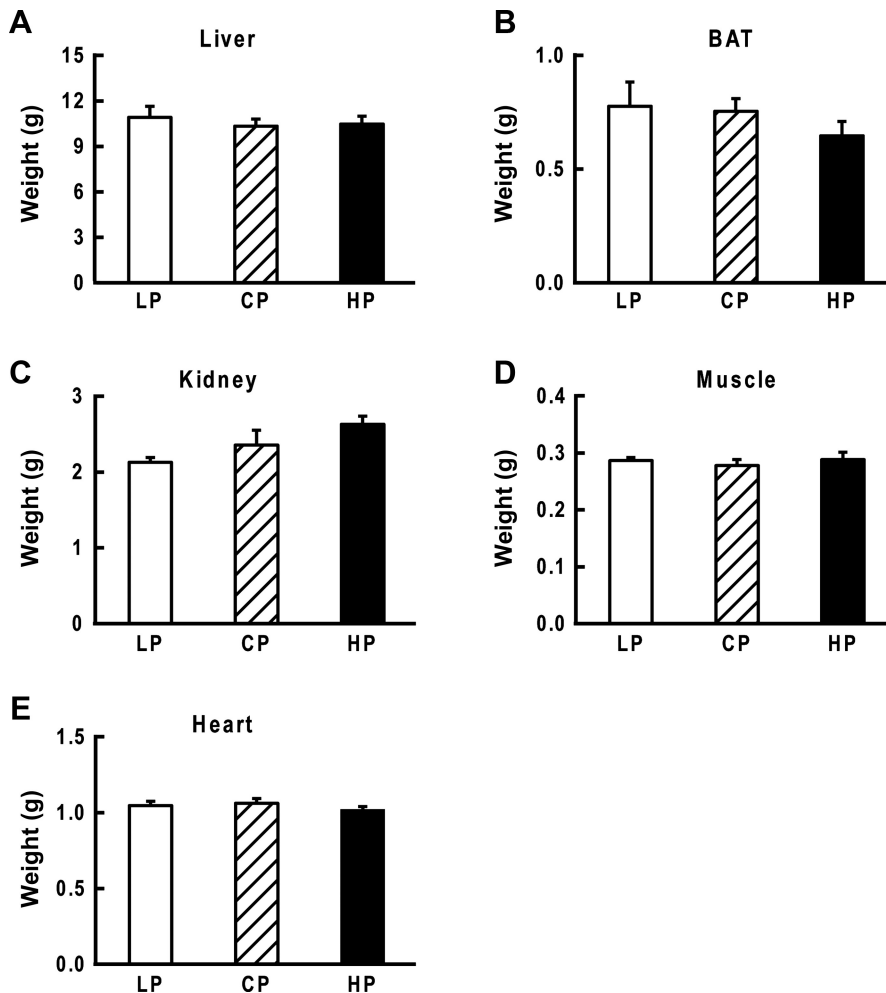

Fig. 2. Organ weight after 4 wk of the experimental diets being fed. At euthanization the organs were harvested and washed in saline, and then organ weight was measured after the saline was removed. BAT, brown adipose tissue.
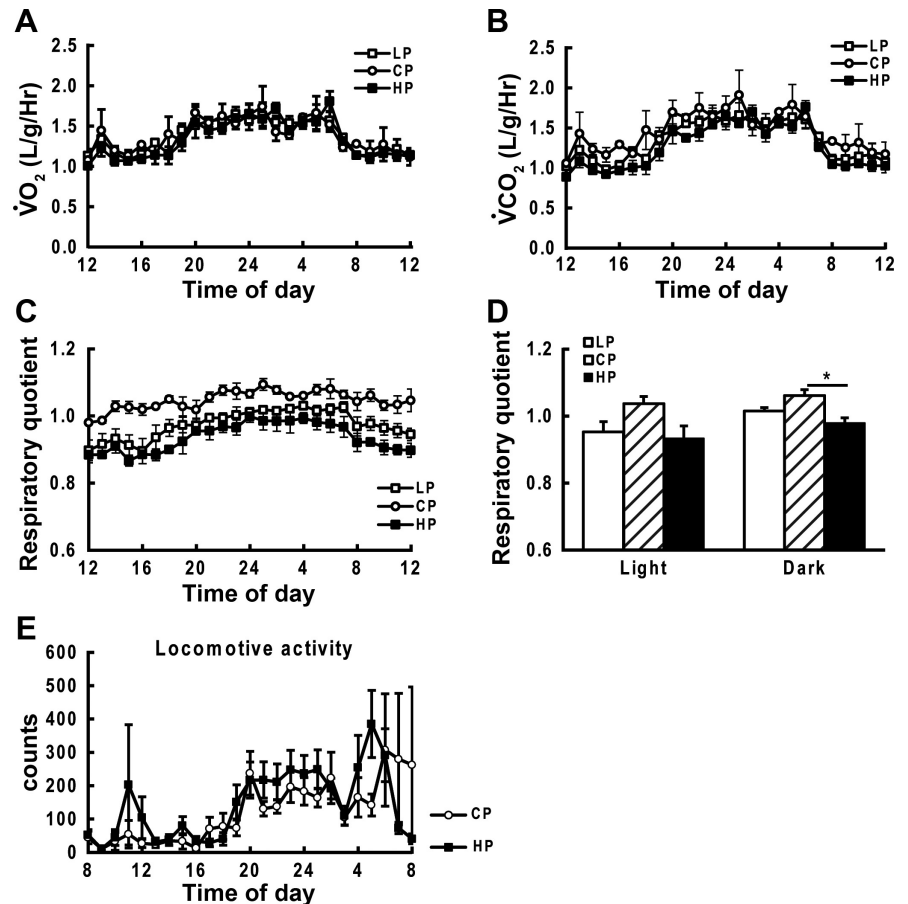
Fig. 3. Effect of dietary P_i on respiratory quotient (RQ) and locomotive activity. *A–C*: oxygen consumption ($\dot{V}O_2$) and CO_2 production ($\dot{V}CO_2$) and RQ ($\dot{V}O_2$/$\dot{V}CO_2$) in rats fed diets containing different amounts of P_i for 3 wk ($n = 3$–4 for each group). Values were collected over a 24-h period. *D*: average value of RQ data in the dark period (8 PM to 8 AM) and the light period (8 AM to 8 PM) were calculated and subjected to the statistical analysis. *E*: measured locomotive activity in CP and HP diet group rats ($n = 6$). Time indicates clock time; 8 AM to 8 PM was the light phase, and 8 PM to 8 AM was the dark phase. Count means average no. across the infrared sensor per hour. Data are presented as means ± SE ($n = 6$). *$P < 0.05$.

the HP group than in the LP group. It was well known that PTH enhances $1,25(OH)_2D$ synthesis as well as calcium reabsorption and P_i excretion in the kidney (26). The increased $1,25(OH)_2D$ levels in the plasma may reflect the sixfold increase in the plasma PTH level in HP group rats (Table 4). On the other hand, the fasting plasma TG, T-Cho levels, and hepatic lipid contents were unchanged, whereas the fasting plasma NEFA levels were significantly decreased in the HP group compared with those of the LP and CP groups (Table 3).

Effect of dietary P_i on glucose tolerance and insulin tolerance in rats. To address the effects of dietary P_i on glucose metabolism in more detail, we also performed an oral glucose tolerance test (OGTT) in these rats after 3 wk of diet intervention. As shown in Fig. 4, there were no significant differences in blood glucose levels among all experimental groups, whereas there was a slight increase in the blood insulin level of LP group rats compared with that of HP group rats. Plasma insulin levels showed peak values in all groups at 15 min after glucose administration (Fig. 4*B*). Additionally, fasting insulin levels were significantly greater in LP group rats than in HP group rats, but there was no difference in fasting blood glucose levels among the groups (Fig. 4, *C* and *D*). To evaluate the degree of insulin resistance, we performed the HOMA-IR and insulin tolerance test. HP group rats had a significantly lower average HOMA-IR score than LP group rats (Fig. 4*E*). Consistent with OGTT results, insulin tolerance test also showed a slightly higher level of glucose in the LP group compared with CP and the HP group (Fig. 4*F*). These data indicate that

increased body fat accumulation in the LP group caused the impaired glucose tolerance and insulin sensitivity.

Effects of dietary P_i on gene expression in the liver and white adipose tissue. The body weight, fat mass, and RQ data suggest that HP diet-fed rats may have had increased fatty acid oxidation, resulting in enhanced energy expenditure and reduced body weight gain. To further explore the responsible tissue, we examined the expression of genes involved in lipogenesis and lipolysis in liver and WAT. Animals fed the HP diet showed a significantly decreased hepatic expression of acetyl-CoA carboxylase (ACC) mRNA (Fig. 5*A*), which is the

Table 3. *Body weight and biomarkers related to glucose and lipid metabolism*

	LP (0.2%)	CP (0.6%)	HP (1.2%)
Body weight, g	361 ± 4.5	352 ± 7.5	345 ± 8.0
NEFA, mEq/l	0.49 ± 0.04[a]	0.47 ± 0.03[a]	0.34 ± 0.02[b]
Triglyceride, mg/dl	168 ± 35	131 ± 19	120 ± 23
Total cholesterol, mg/dl	61.2 ± 12.9	48.6 ± 4.0	57.3 ± 4.9
Liver triglyceride, mg/g	3.03 ± 0.7	2.6 ± 0.2	3.2 ± 0.6
Liver cholesterol, mg/g	0.36 ± 0.05	0.39 ± 0.03	0.45 ± 0.05
Free T_3, pg/ml	3.1 ± 0.2	3.1 ± 0.1	2.8 ± 0.3
Free T_4, ng/dl	2.5 ± 0.1	2.8 ± 0.2	2.7 ± 0.2

All data are presented as means ± SE. NEFA, nonesterified fatty acids; T_3, triiodothyronine; T_4, thyroxine 4. Blood and urine sampling was performed at euthanization under fasting conditions at 4 wk after the experimental diet period was started. Values with superscripts of a common letter differ significantly ($P < 0.05$; $n = 6$ for each group).

Table 4. *Biomarker levels related to P_i metabolism*

Plasma	LP (0.2%)	CP (0.6%)	HP (1.2%)
P_i, mg/dl	6.32 ± 0.3	5.84 ± 0.4	5.37 ± 0.48
Calcium, mg/dl	8.9 ± 0.7	9.04 ± 1.2	8.81 ± 1.2
PTH, pg/ml	40 ± 10.9[a]	40 ± 12.6[a]	256.4 ± 75.7[b]
FGF23, pg/ml	228 ± 29.2	231 ± 47.6	408 ± 82.6
1,25(OH)$_2$D, pg/ml	217 ± 20.3[a]	294 ± 24.9	377 ± 28.3[b]
Creatinine, mg/dl	1.03 ± 0.06	0.88 ± 0.10	1.01 ± 0.22
BUN, mg/dl	12.4 ± 0.65[a]	12.8 ± 0.5[a]	16.9 ± 1.6[b]
Urine P_i, mg/dl	32.3 ± 11.3[a]	407 ± 87.9[b]	930 ± 89.2[c]
Urine calcium, mg/dl	9.23 ± 2.7	7.22 ± 2.1	6.3 ± 2.1

All data are presented as means ± SE. BUN, blood urea nitrogen; PTH, parathyroid hormone; 1,25(OH)$_2$D, 1,25-dihydroxyvitamin D; FGF23, fibroblast growth factor 23. Blood and urine sampling were performed at euthanization under fasting conditions during a 4-wk period. Values marked with superscripts of a common letter differ significantly ($P < 0.05$; $n = 6$ for each group).

rate-limiting enzyme for fatty acid synthesis (18). Sterol regulatory element-binding protein-1c (SREBP-1c) and fatty acid synthase (FAS) mRNA levels also tended to be lower in HP group rats than in LP group rats, but without statistical significance (Fig. 5, *B* and *C*). On the contrary, the mRNA expression of PGC-1α, which regulates genes involved in lipid oxidation and energy homeostasis (21), was slightly increased

in HP group rats, but no significant differences in PGC-1α expression were identified among groups (Fig. 5*D*). Carnitine palmitoyl transferase 1 and UCP2 mRNA levels in the liver were also not changed (Fig. 6). On the other hand, the lowered plasma NEFA level in HP group rats (Table 3) suggests that fatty acid utilization was increased in WAT of this group. Unexpectedly, the mRNA level of hormone-sensitive lipase, which is a key enzyme for fatty acid mobilization (22) in WAT, was not different among the groups (Fig. 5*G*). The expression levels of the lipogenesis-related genes we investigated, such as ACC (Fig. 5*E*) and SREBP-1c (Fig. 5*F*), were also not different among groups in WAT, and the expression levels of PGC-1α also did not differ among groups in WAT (Fig. 5*H*). These observations indicate that repressed fat accumulation in HP group rats may have been a result of reduced lipogenesis in the liver, but the results do not indicate increased fat oxidation in liver or WAT.

Effect of dietary P_i on gene expression in brown adipose tissue. Next, we analyzed the BAT, which contributes significantly to the control of body temperature and energy expenditure (10). BAT weight was reduced in HP group rats compared with that of LP group (Fig. 2). Expression of FAS mRNA was significantly lower in HP group rats than in LP group rats (Fig. 7*A*), but there was no significant difference in
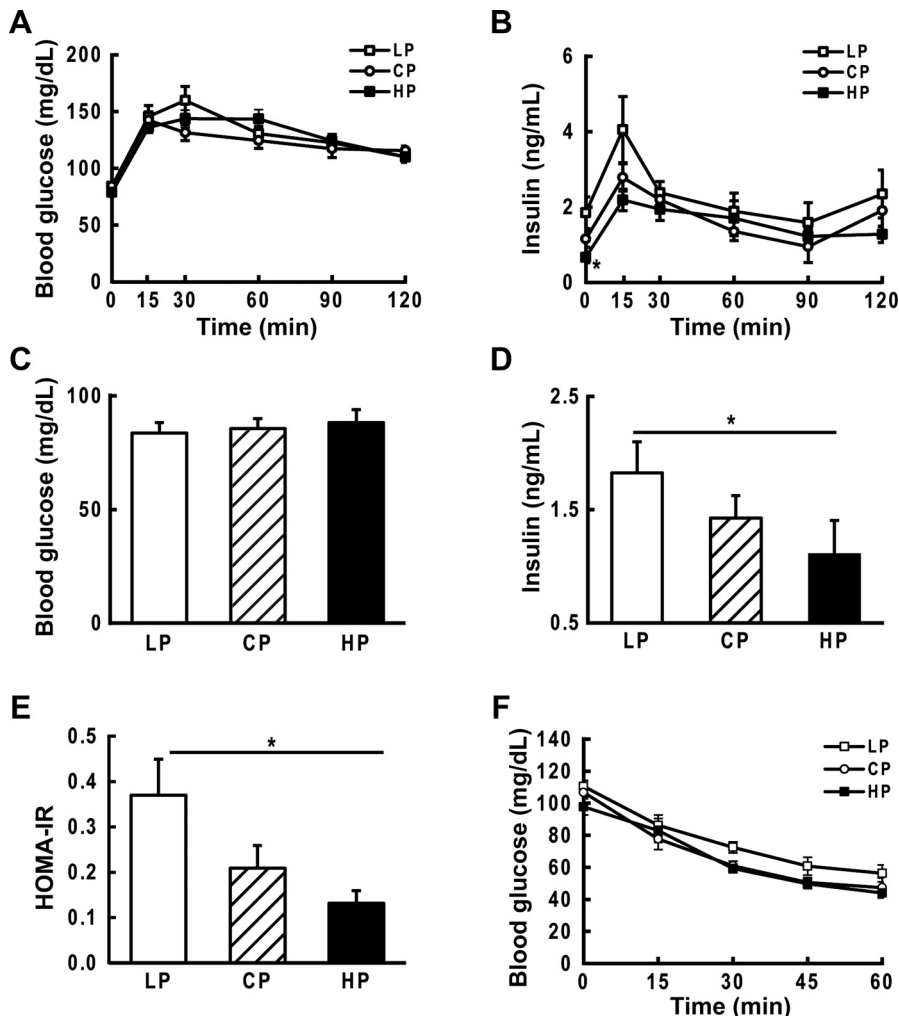

Fig. 4. Effect of dietary P_i on oral glucose and insulin tolerance. *A* and *B*: after being fasted for 14–16 h, the rats were given an oral dose of 2 g/kg body wt. Blood samples were taken at 0, 15, 30, 60, 90, and 120 min after glucose administration. Blood glucose (*A*) and insulin (*B*) levels measured after the feeding of diets containing different amounts of P_i for 3 wk ($n = 5$ for each group). *C*–*E*: concentrations of fasting glucose (*C*) and insulin (*D*) and homeostasis model assessment of insulin resistance (HOMA-IR) score. *F*: insulin tolerance test was performed at 3 wk. Insulin (0.75 U/kg BW) was administrated intreperitoneally to the unanesthetized rats. Data are presented as means ± SE ($n = 6$). *$P < 0.05$.
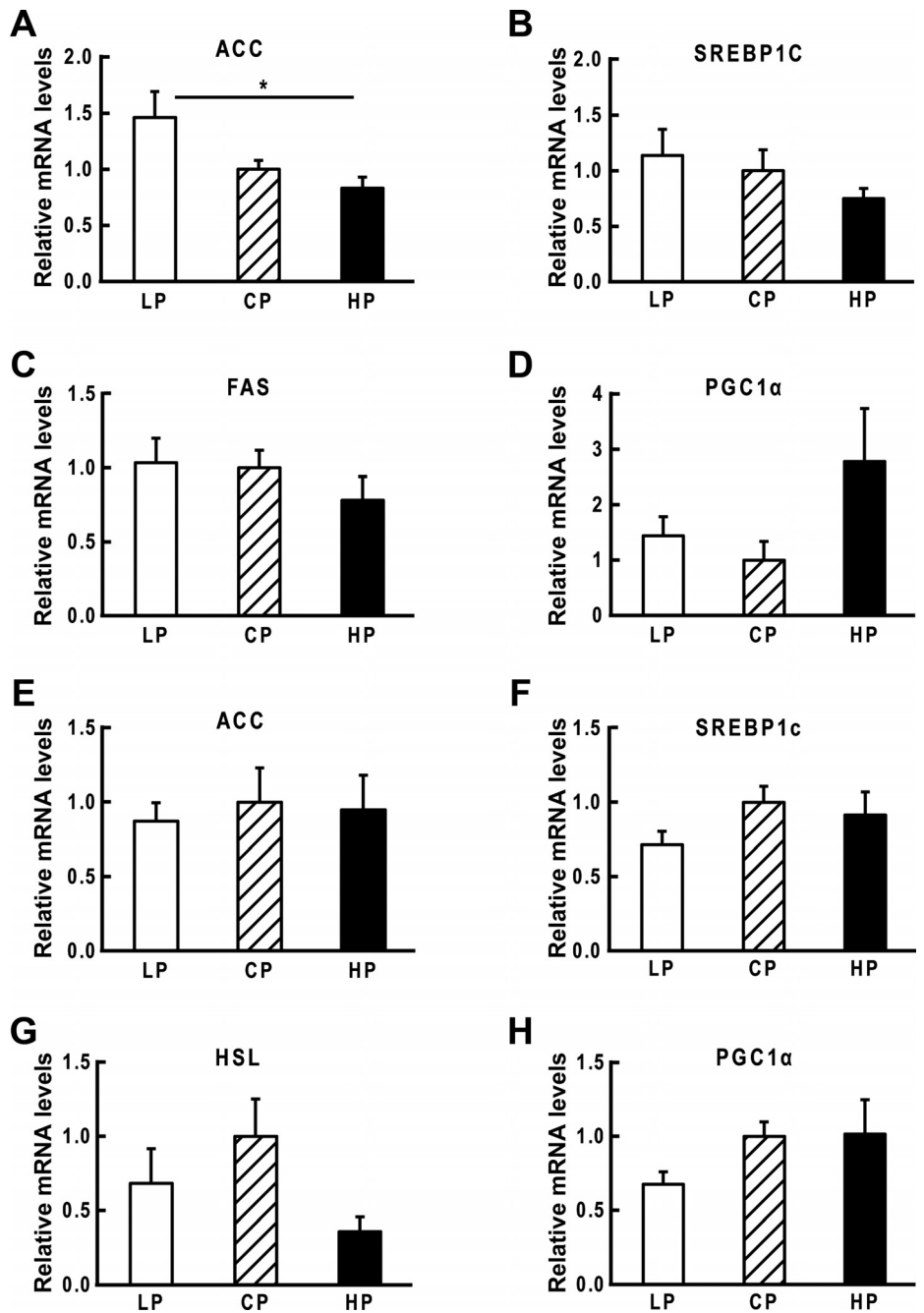
Fig. 5. Effects of dietary P_i on gene expression in the liver and white adipose tissues. Hepatic (A–D) and white adipose tissue (E–H) gene expression at 4 wk after the experimental diets were started. mRNA expression levels were determined by quantitative RT-PCR analysis. The ratio for the data from the CP group was arbitrarily set at 1. Genes related to lipogenesis include ACC (acetyl-CoA carboxylase), FAS (fatty acid synthase), and SREBP-1c (sterol regulatory element-binding protein-1c). Genes related to fatty acid oxidation include PGC-1α (peroxisome proliferator-activated receptor-γ coactivator-1α) and HSL (hormone-sensitive lipase). Data are presented as means ± SE ($n = 6$). *$P < 0.05$.

SREBP-1c mRNA expression in BAT (Fig. 7B). Surprisingly, expression of UCP1 mRNA, which encodes a BAT-specific thermogenic protein, was dramatically increased in HP group rats compared with that in LP and CP group rats (Fig. 7C). PGC-1α mRNA expression in the BAT of HP group rats was also higher than that of LP and CP group rats (Fig. 7D). This finding was consistent with a low RQ level in HP group rats. These results suggest that upregulation of UCP1 and PGC-1α expression in BAT must be related to the decreased fat accumulation and increased BAT activation in the HP group.

Effect of dietary P_i on [18F]FDG uptake in BAT and quantitative kinetic modeling. Recent studies have reported that the assessment of BAT metabolic activity using [18F]FDG PET/CT was a feasible and reliable method. Following these

reports, we investigated the effect of dietary P_i on [18F]FDG uptake using PET/CT imaging in BAT. Unexpectedly, PET/CT images revealed no significant [18F]FDG uptake in the BAT of all groups at ambient temperature (Fig. 8A). Quantitative analysis of the [18F]FDG SUV of BAT also showed no significant difference among the groups (Fig. 8, B and C). Baba et al. (3) reported previously that the CT HU value of BAT was increased in activated conditions in both animals and patients. The CT HU value of BAT was calculated manually by linear interpolation of water CT density (assuming CT HU = 0) using image analysis software (Fig. 8, D and E). The CT HU value of the BAT of HP group rats was decreased compared with that of the LP group. The change in the CT HU value was specific to BAT and related to the physiological alterations in this
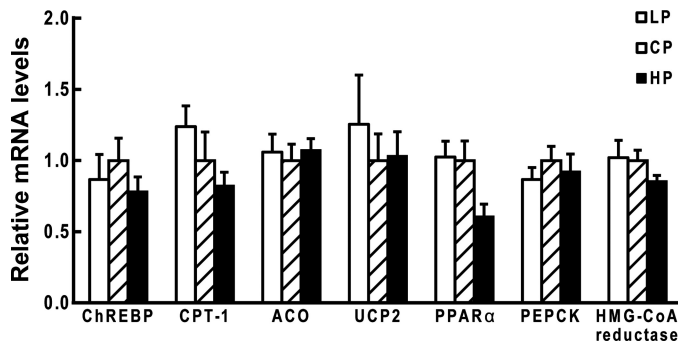
Fig. 6. Effect of dietary P_i on gene expression in the liver. Hepatic gene expression levels at 4 wk of the experimental diets being fed. The mRNA expression levels were determined by quantitative RT-PCR analysis. The ratio for the data from the CP group was arbitrarily set at 1. ChREBP, carbohydrate-responsive element-binding protein; CPT-1, carnitine palmitoyltransferase 1; ACO, acyl-CoA oxidase; UCP2, uncoupling protein 2; PPARα, peroxisome proliferator-activated receptor-α; PEPCK, phospho*enol*pyruvate carboxykinase; HMG-CoA reductase, hydroxymethylglutaryl-CoA reductase.

tissue. Our histological analysis of BAT revealed that the lipid content of BAT was decreased in the HP group (Fig. 8*F*), indicating that the changes in the CT HU value may have reflected alterations in BAT volume. Because we did not find any differences in FDG uptake in BAT among groups, we performed further examinations using kinetic modeling (Fig. 9). Kinetic modeling allowed quantification of the kinetic parameters k_1, k_2, k_3, and k_i in BAT. No significant differences were observed among groups in the averages of the FDG transport parameters k_1 and k_2 on the 4th wk of the experimental diet period (Fig. 9, *A* and *B*). Hexokinase activity (k_3) and the BAT net influx rate constant (k_i) for glucose were significantly smaller in the HP group than in the other groups (Fig. 9, *C* and *D*), showing that these parameters can be altered depending on the amount of P_i content in the diet. The kinetic data also indicated a significant decrease in FDG uptake in the HP group when compared with the other groups on the 4th wk of the experimental diet period.

These data suggested that a HP diet may be implicated in inhibiting glucose uptake in BAT.

Effect of P_i stimulation on UCP1 expression in brown adipocytes. To gain further understanding of the mechanisms involved in dietary high-P_i-induced UCP1 expression in BAT, we investigated the effects of P_i and P_i-regulating hormones on the expression of UCP1 mRNA in HB2 cells. First, we examined whether elevation of extracellular P_i concentration could induce the expression of UCP1 mRNA in HB2 cells. As shown in Fig. 10*A*, the increase in P_i concentration did not affect the mRNA expression levels of UCP1. We also tested the effect of PTH on the expression of UCP1 mRNA in HB2 cells. Adipose tissue can express PTH receptor (27). In addition, PTH receptor is a G protein-coupled receptor that activates the cyclic AMP-dependent protein kinase pathway (47). So we hypothesized that high plasma levels of PTH in the HP group can induce the PKA signaling pathway, thereby promoting UCP1 expression. As shown in Fig. 10*B*, however, PTH did not affect the expression of the mRNA. Finally, we also examined the effect of FGF23, which is an important phosphaturic factor, on the expression of UCP1 mRNA in HB2 cells. As also shown in Fig. 10*C* is that FGF23 did not affect the expression of mRNA in HB2 cells (Fig. 10*C*). These data indicate that elevated serum P_i concentration and the P_i-regulating hormones PTH and FGF23 did not directly affect the BAT activity in the HP group.

DISCUSSION

In the present study, we investigated the effects of dietary P_i on glucose and lipid metabolism. The HP diet group showed a gradual and significant suppression of body weight gain until the 14th wk of the experimental diet period, although food intake was similar to that in other diet groups. A slight suppression of body weight gain by the HP diet was observed on the 4th wk. We hypothesized that a metabolic change had arisen on the 4th wk in the HP diet-fed rats. We found that ingestion of the HP diet for 4 wk reduced visceral fat mass but
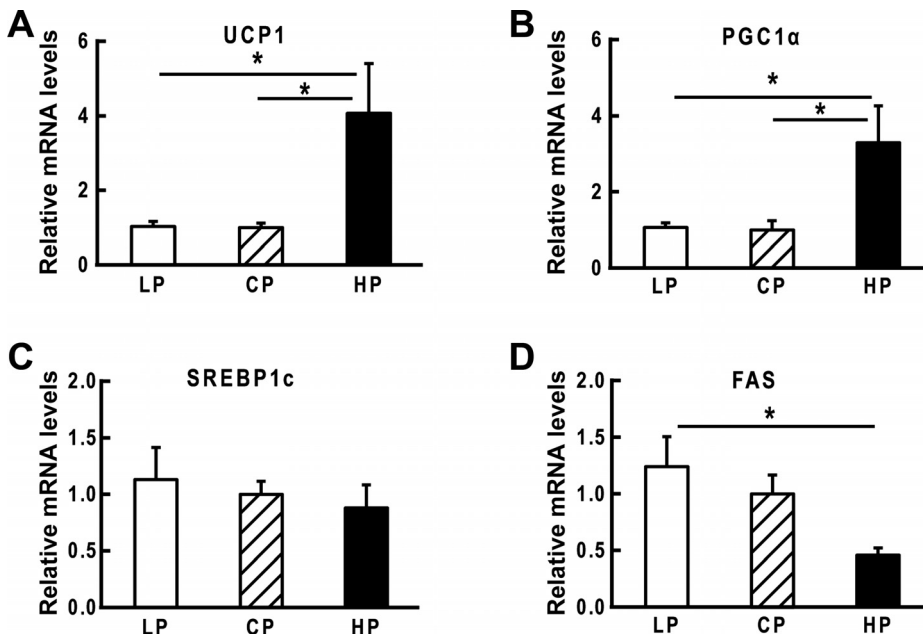

Fig. 7. Effect of dietary P_i on gene expression BAT. Gene expression in BAT at 4 wk after the experimental diet period was started. The mRNA expression levels were determined by quantitative RT-PCR analysis. The ratio for the data from the CP group was arbitrarily set at 1. *A*: UCP1. *B*: PGC-1α. *C*: SREBP-1c. *D*: FAS. Data are presented as means ± SE ($n = 6$). *$P < 0.05$.
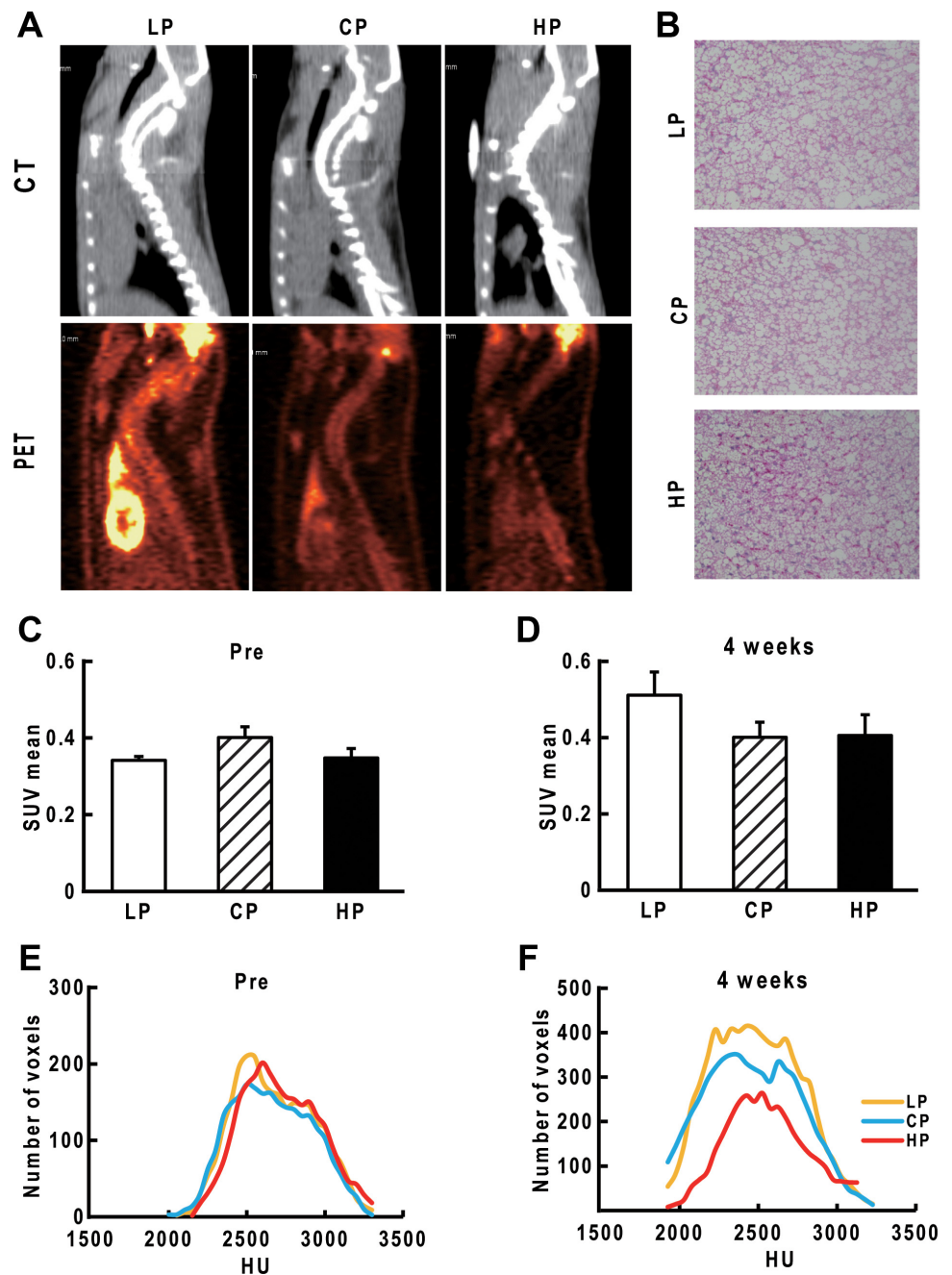
Fig. 8. Sagittal views and quantitative analysis of PET/CT images. *A*: sagittal views of PET/CT images, LP (*left*), CP (*middle*), and HP (*right*), showing intense [^{18}F]fludeoxyglucose ([^{18}F]FDG) uptake in the BAT. *B*: hematoxylin and eosin-stained tissue sections from intracellular BAT. *C* and *D*: quantitative analysis of [^{18}F]FDG uptake obtained from PET/CT images for BAT in 3 groups, prefeeding (*C*) and at 4 wk after starting the experimental diet period (*D*). *E* and *F*: differences between the BAT and WAT volumes of interest based on CT data [Hounsfield unit (HU)], prefeeding (*E*), and at 4 wk (*F*). Data are presented as means ± SE (*n* = 6). SUV, standard uptake value.

did not result in differences in the weights of liver, muscle, or other organs. We demonstrated that rats fed the HP diet showed decreased visceral fat mass and altered mRNA expression levels of lipogenesis-related genes such as ACC, FAS, and SREBP-1c in the liver. Furthermore, low RQ value in the HP group may be involved in the low fat accumulation. On the other hand, fat accumulation and impaired glucose tolerance/insulin sensitivity was observed in the LP group.

The significant reductions in visceral fat accumulation found in HP group rats may be due to enhanced basal metabolism. Our data indicated that HP diet intake led to a preferential utilization of fat for energy production, because we demonstrated lowered levels of the respiratory quotient ($\dot{V}_{CO_2}/\dot{V}_{O_2}$) in the HP group compared with the CP diet group without

changes in locomotive activity. The suppressed fat mass could also be due to the reduced expression of hepatic lipogenic genes such as SREBP-1c, FAS, and ACC, whereas the expression levels of fat oxidation-related genes were not changed. Decreased fasting NEFA levels in the HP group rats suggested that most of the released NEFA were utilized for β-oxidation in the liver, BAT, or skeletal and cardiac muscles, although we did not directly evaluate lipolysis or β-oxidation in the muscle. Our data indicate at least in part that increased fat oxidation in BAT was primarily responsible for the decrease in visceral fat accumulation observed in HP diet-fed rats.

Body fat accumulation was regulated by various hormones such as insulin, leptin, and adiponectin. Leptin is a key regulator for the regulation of body mass and is produced almost
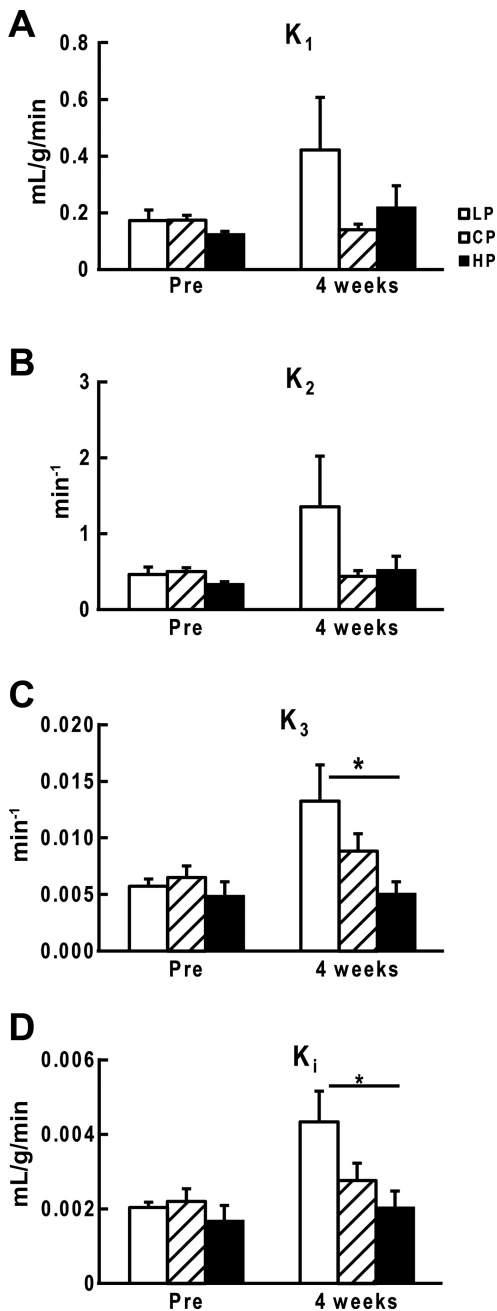
Fig. 9. Quantitative kinetic modeling for BAT. *A–D*: quantification of the kinetic parameters k_1 (*A*), k_2 (*B*), k_3 (*C*), and k_i (*D*) in BAT; data for before feeding and at 4 wk of feeding with the experimental diets. Data are presented as means $\pm$ SE ($n = 6$), *$P < 0.05$.

the HP diet in the decreased fat accumulation. Fasting plasma insulin level, HOMA-IR, and insulin tolerance test demonstrated that LP diet was involved in the insulin-resistant state, which was probably due to fat accumulation. We did not observe any significant difference between HP diet and CP diet groups, although low fat accumulation and body weight gain were observed. Greater dietary P_i intake in humans can increase the circulating levels of PTH and FGF23 (2, 51). These hormones reduce P_i concentration mainly by enhancing its renal excretion. It has been proposed that insulin sensitivity and HOMA-IR correlate inversely with plasma PTH (11) and FGF23 (49) in obese adults, suggesting that increased PTH and FGF23 levels may be associated with metabolic disorders. The more detailed mechanism of the effects of HP diet on glucose and lipid metabolisms must be investigated in a future study.

Furthermore, high dietary P_i intake was associated with increased left ventricular mass (50). Although the detailed mechanism has not been clarified, elevated FGF23 resulting from intake of a diet with a high P_i content may lead to increased left ventricular mass. Faul et al. (15) demonstrated that FGF23 can influence left ventricular hypertrophy. An increase in left ventricular mass is also related to cardiovascular complications such as arrhythmia and heart failure. Interestingly, studies in human and animal models have suggested that insulin resistance and fat oxidation are improved in failed hearts (12, 37). Although energy metabolism was increased by cardiac hypertrophy, there were no significant changes in heart mass in our HP diet-fed rats. Additionally, our experiment demonstrated that neither PTH nor FGF23 increased the expression of UCP1 mRNA in HB2 cells, indicating that the induced UCP1 mRNA expression by ingestion of high dietary P_i may be due to other mechanisms, including the sympathetic nervous system.

BAT is known to play an important role in fat oxidation by regulating thermogenesis (10, 28), which is mediated by its characteristic protein UCP1 (33). The importance of UCP1, the major uncoupling protein isoform expressed in BAT, has been understood in the development of obesity in UCP1-ablated mice (16). Furthermore, upregulated UCP1 expression was reported to result in increased thermogenesis and energy expenditure, which helps to protect from obesity and fat accumulation (29). This upregulation of UCP1 can be mediated by the transcriptional factor PGC-1α (21, 30). In our study, a consistently high level of PGC-1α mRNA expression was observed in HP group rats, suggesting that thermogenesis was increased in the BAT of these animals. However, it remains unclear how a high-P_i diet can affect UCP1 expression in BAT. NEFAs in serum are normally rapidly taken up by BAT, and HP diet intake should stimulate UCP1 expression to increase thermogenesis and energy expenditure in BAT, as described in another study (33).

Measuring the metabolic activity of BAT is important for the development of novel strategies for the evaluation of energy expenditure. Glucose uptake by BAT is increased when it becomes metabolically active (38). Unexpectedly, dietary P_i had no effect on FDG uptake in BAT. This finding was possibly because of the following reasons: *1*) low plasma insulin level (as discussed above, low fasting plasma insulin level may explain low glucose uptake in BAT in HP diet group; however, the insulin level was significantly different between LP diet and HP diet groups but not CP diet and HP diet group);

exclusively by adipose tissue (13, 25). Serum leptin levels have been reported to show a positive correlation with adiposity. In our study, the decreased leptin level in the HP group may reflect the decreased fat mass. We also observed a low plasma level of insulin in the HP group compared with the LP group but not the CP group; this may contribute to decreased visceral fat mass, since insulin increases glucose uptake in muscle and fat and inhibits lipolysis (41). However, this study did not evaluate insulin signaling, and so further investigation will be required to determine the relative contributions of the altered plasma levels of leptin and insulin resulting from feeding with

Fig. 10. Effect of P_i, parathyroid hormone (PTH) and fibroblast growth factor 23 (FGF23) on the UCP1 expression in brown adipocytes HB2 cells. After 2 days of induction and differentiation, the cells were cultured in differentiation medium containing control (0.9 mM P_i), 2 mM P_i, or 3 mM P_i for 6 days (*A*), differentiation medium supplemented with human fragment PTH concentration [0 (control), 10, and 50 ng/ml; *B*], or supplement with recombinant human FGF23 concentration [0, 10, and 20 ng/ml for 6 days; *C*]. After treatment with P_i, PTH, or FGF23 for 6 days, the cells were harvested, and total RNA was extracted. The expression levels of UCP1 mRNA was determined by real-time PCR analysis. The ratio for the data from the control was arbitrarily set at 1. Data are presented as means $\pm$ SE ($n = 4$).
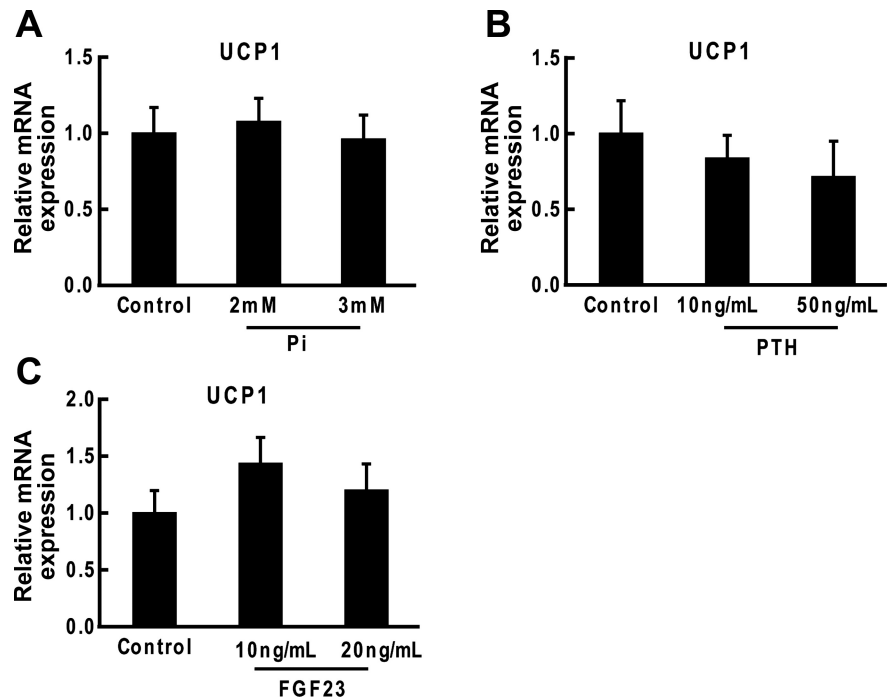
2) ambient temperature (the influence of exposure to cold on BAT activity is potentially important for the interpretation of FDG PET/CT studies) (3); or *3*) pharmacological stimulants (to active BAT at ambient temperatures, it was necessary to stimulate the noradrenergic receptors). These reasons may be implicated in the low FDG uptake in all groups. In this study, BAT did not receive any stimuli to activate glucose uptake. Although we did not observe FDG accumulation in our study, it was most likely activated because HP group rats exhibited higher body temperatures (HP vs. LP: 34.1 ± 0.7 vs. $33.3 \pm 0.4°C$). BAT takes up glucose for oxidation, and its utilization of glucose is increased under thermogenic conditions. Some studies have pointed out that glucose uptake in BAT may not always reflect its thermogenic activity, since glucose taken up by this tissue is used predominantly for lipogenesis (31), and its uptake is dependent on intracellular TG content (9). Moreover, thermogenic activity is regulated mainly by the sympathetic nervous system, which innervates mostly BAT. The main fuel for this heat generation in BAT is fatty acids, which provide most of the energy for heat production (20). In healthy men, BAT can significantly contribute to cold-induced thermogenesis and is fueled mostly by fatty acids (4, 39). In here, the HP group showed inhibited hexokinase (HK) activities, as measured by decreases in the kinetic parameters k_3 and k_i. As mentioned above, reduction of glucose uptake by inhibition of HK activity in the HP group may also increase fatty acids utilization in BAT, and this interpretation is supported by our histological analysis of BAT and kinetic analysis data; however, we did not examine NEFA uptake or fatty acid transport in BAT. Our data imply that a high-P_i diet may suppress glucose uptake and increase fatty acid utilization in BAT of the rats.

Another unexpected result was that the LP group did not increase RQ value, although impaired glucose tolerance/insulin sensitivity and fat accumulation were observed as reported previously (14). Increases in plasma leptin level and impairment of glucose tolerance/insulin sensitivity resulted from increased fat accumulation. Although fat accumulation increased in the LP group, the expressions of UCP1 and PGC-1α mRNA and RQ value in the LP group were not increased. Further investigation will be needed to clarify the effect of dietary P_i restriction on glucose and lipid metabolism.

In conclusion, we demonstrated that administration of a high-P_i diet decreased visceral fat mass via increased fat oxidation and suppressed fatty acid synthesis as well as increased UCP1 mRNA expression in BAT. The physiological importance of the effects of a high P_i diet on energy metabolism should be clarified in a future study.

DISCLOSURES

No conflicts of interest, financial or otherwise, are declared by the authors.

AUTHOR CONTRIBUTIONS

M.A., H.O., H.Y., E.T., and Y.T. conception and design of research; M.A., H.O., T.O., H.K., H.U., Y.K., H.S., and Y.T. performed experiments; M.A., H.O., T.O., H.K., H.U., Y.K., M.M., H.Y.-O., H.S., H.Y., and Y.T. analyzed data; M.A., H.O., T.O., H.K., H.U., Y.K., M.M., H.Y.-O., H.S., H.Y., E.T., and Y.T. interpreted results of experiments; M.A., H.O., T.O., H.K., H.U., M.M., H.Y., and Y.T. prepared figures; M.A., H.O., H.Y., E.T., and Y.T. drafted manuscript; M.A., H.K., M.M., H.Y.-O., H.S., H.Y., E.T., and Y.T. edited and

revised manuscript; M.A., H.O., T.O., H.K., H.U., Y.K., M.M., H.Y.-O., H.S., H.Y., E.T., and Y.T. approved final version of manuscript.

REFERENCES

1. **Abramowitz M, Muntner P, Coco M, Southern W, Lotwin I, Hostetter TH, Melamed ML.** Serum alkaline phosphatase and phosphate and risk of mortality and hospitalization. *Clin J Am Soc Nephrol* 5: 1064–1071, 2010.

2. **Antoniucci DM, Yamashita T, Portale AA.** Dietary phosphorus regulates serum fibroblast growth factor-23 concentrations in healthy men. *J Clin Endocrinol Metab* 91: 3144–3149, 2006.

3. **Baba S, Engles JM, Huso DL, Ishimori T, Wahl RL.** Comparison of uptake of multiple clinical radiotracers into brown adipose tissue under cold-stimulated and nonstimulated conditions. *J Nucl Med* 48: 1715–1723, 2007.

4. **Bartelt A, Bruns OT, Reimer R, Hohenberg H, Ittrich H, Peldschus K, Kaul MG, Tromsdorf UI, Weller H, Waurisch C, Eychmüller A, Gordts PL, Rinninger F, Bruegelmann K, Freund B, Nielsen P, Merkel M, Heeren J.** Brown adipose tissue activity controls triglyceride clearance. *Nat Med* 17: 200–205, 2011.

5. **Benz MR, Czernin J, Allen-Auerbach MS, Dry SM, Sutthiruangwong P, Spick C, Radu C, Weber WA, Tap WD, Eilber FC.** 3′-deoxy-3′-[18F]fluorothymidine positron emission tomography for response assessment in soft tissue sarcoma: a pilot study to correlate imaging findings with tissue thymidine kinase 1 and Ki-67 activity and histopathologic response. *Cancer* 118: 3135–3144, 2012.

6. **Bergwitz C, Jüppner H.** Regulation of phosphate homeostasis by PTH, vitamin D, and FGF23. *Annu Rev Med* 61: 91–104, 2010.

7. **Block GA, Ix JH, Ketteler M, Martin KJ, Thadhani RI, Tonelli M, Wolf M, Jüppner H, Hruska K, Wheeler DC.** Phosphate homeostasis in CKD: report of a scientific symposium sponsored by the National Kidney Foundation. *Am J Kidney Dis* 62: 457–473, 2013.

8. **Block GA, Klassen PS, Lazarus JM, Ofsthun N, Lowrie EG, Chertow GM.** Mineral metabolism, mortality, and morbidity in maintenance hemodialysis. *J Am Soc Nephrol* 15: 2208–2218, 2004.

9. **Blondin DP, Labbé SM, Tingelstad HC, Noll C, Kunach M, Phoenix S, Guérin B, Turcotte EE, Carpentier AC, Richard D, Haman F.** Increased brown adipose tissue oxidative capacity in cold-acclimated humans. *J Clin Endocrinol Metab* 99: E438–E446, 2014.

10. **Cannon B, Nedergaard J.** Brown adipose tissue: function and physiological significance. *Physiol Rev* 84: 277–359, 2004.

11. **Chiu KC, Chuang LM, Lee NP, Ryu JM, McGullam JL, Tsai GP, Saad MF.** Insulin sensitivity is inversely correlated with plasma intact parathyroid hormone level. *Metabolism* 49: 1501–1505, 2000.

12. **Chokshi A, Drosatos K, Cheema FH, Ji R, Khawaja T, Yu S, Kato T, Khan R, Takayama H, Knöll R, Milting H, Chung CS, Jorde U, Naka Y, Mancini DM, Goldberg IJ, Schulze PC.** Ventricular assist device implantation corrects myocardial lipotoxicity, reverses insulin resistance, and normalizes cardiac metabolism in patients with advanced heart failure. *Circulation* 125: 2844–2853, 2012.

13. **Dencker M, Thorsson O, Karlsson MK, Lindén C, Wollmer P, Ahrén B.** Leptin is closely related to body fat in prepubertal children aged 8–11 years. *Acta Paediatr* 95: 975–979, 2006.

14. **Ellam T, Wilkie M, Chamberlain J, Crossman D, Eastell R, Francis S, Chico TJ.** Dietary phosphate modulates atherogenesis and insulin resistance in apolipoprotein E knockout mice—brief report. *Arterioscler Thromb Vasc Biol* 31: 1988–1990, 2011.

15. **Faul C, Amaral AP, Oskouei B, Hu MC, Sloan A, Isakova T, Gutiérrez OM, Aguillon-Prada R, Lincoln J, Hare JM, Mundel P, Morales A, Scialla J, Fischer M, Soliman EZ, Chen J, Go AS, Rosas SE, Nessel L, Townsend RR, Feldman HI, St John Sutton M, Ojo A, Gadegbeku C, Di Marco GS, Reuter S, Kentrup D, Tiemann K, Brand M, Hill JA, Moe OW, Kuro-O M, Kusek JW, Keane MG, Wolf M.** FGF23 induces left ventricular hypertrophy. *J Clin Invest* 121: 4393–4408, 2011.

16. **Feldmann HM, Golozoubova V, Cannon B, Nedergaard J.** UCP1 ablation induces obesity and abolishes diet-induced thermogenesis in mice exempt from thermal stress by living at thermoneutrality. *Cell Metab* 9: 203–209, 2009.

17. **Folch J, Lees M, Sloane Stanley GH.** A simple method for the isolation and purification of total lipides from animal tissues. *J Biol Chem* 226: 497–509, 1957.

18. **Fukuda N, Ikawa Y, Aoyagi T, Kozaki A.** Expression of the genes coding for plastidic acetyl-CoA carboxylase subunits is regulated by a location-sensitive transcription factor binding site. *Plant Mol Biol* 82: 473–483, 2013.

19. **Grima P, Guido M, Chiavaroli R, Stano F, Tundo P, Tana M, de Donno A, Zizza A.** Altered phosphate metabolism in HIV-1-infected patients with metabolic syndrome. *Scand J Infect Dis* 44: 133–137, 2012.

20. **Haman F, Péronnet F, Kenny GP, Massicotte D, Lavoie C, Scott C, Weber JM.** Effect of cold exposure on fuel utilization in humans: plasma glucose, muscle glycogen, and lipids. *J Appl Physiol (1985)* 93: 77–84, 2002.

21. **Handschin C, Spiegelman BM.** Peroxisome proliferator-activated receptor gamma coactivator 1 coactivators, energy homeostasis, and metabolism. *Endocr Rev* 27: 728–735, 2006.

22. **Holm C, Osterlund T, Laurell H, Contreras JA.** Molecular mechanisms regulating hormone-sensitive lipase and lipolysis. *Annu Rev Nutr* 20: 365–393, 2000.

23. **Håglin L.** Hypophosphataemia: cause of the disturbed metabolism in the metabolic syndrome. *Med Hypotheses* 56: 657–663, 2001.

24. **Irie Y, Asano A, Cañas X, Nikami H, Aizawa S, Saito M.** Immortal brown adipocytes from p53-knockout mice: differentiation and expression of uncoupling proteins. *Biochem Biophys Res Commun* 255: 221–225, 1999.

25. **Janeckova R.** The role of leptin in human physiology and pathophysiology. *Physiol Res* 50: 443–459, 2001.

26. **Janulis M, Wong MS, Favus MJ.** Structure-function requirements of parathyroid hormone for stimulation of 1,25-dihydroxyvitamin D3 production by rat renal proximal tubules. *Endocrinology* 133: 713–719, 1993.

27. **Kir S, White JP, Kleiner S, Kazak L, Cohen P, Baracos VE, Spiegelman BM.** Tumour-derived PTH-related protein triggers adipose tissue browning and cancer cachexia. *Nature* 513: 100–104, 2014.

28. **Klingenspor M.** Cold-induced recruitment of brown adipose tissue thermogenesis. *Exp Physiol* 88: 141–148, 2003.

29. **Li B, Nolte LA, Ju JS, Han DH, Coleman T, Holloszy JO, Semenkovich CF.** Skeletal muscle respiratory uncoupling prevents diet-induced obesity and insulin resistance in mice. *Nat Med* 6: 1115–1120, 2000.

30. **Lowell BB, Spiegelman BM.** Towards a molecular understanding of adaptive thermogenesis. *Nature* 404: 652–660, 2000.

31. **Ma SW, Foster DO.** Uptake of glucose and release of fatty acids and glycerol by rat brown adipose tissue in vivo. *Can J Physiol Pharmacol* 64: 609–614, 1986.

32. **Malik S, Wong ND, Franklin SS, Kamath TV, L'Italien GJ, Pio JR, Williams GR.** Impact of the metabolic syndrome on mortality from coronary heart disease, cardiovascular disease, and all causes in United States adults. *Circulation* 110: 1245–1250, 2004.

33. **Matthias A, Ohlson KB, Fredriksson JM, Jacobsson A, Nedergaard J, Cannon B.** Thermogenic responses in brown fat cells are fully UCP1-dependent. UCP2 or UCP3 do not substitute for UCP1 in adrenergically or fatty scid-induced thermogenesis. *J Biol Chem* 275: 25073–25081, 2000.

34. **Mirbolooki MR, Constantinescu CC, Pan ML, Mukherjee J.** Targeting presynaptic norepinephrine transporter in brown adipose tissue: a novel imaging approach and potential treatment for diabetes and obesity. *Synapse* 67: 79–93, 2013.

35. **Mizuma H, Shukuri M, Hayashi T, Watanabe Y, Onoe H.** Establishment of in vivo brain imaging method in conscious mice. *J Nucl Med* 51: 1068–1075, 2010.

36. **Nemere I.** The ins and outs of phosphate homeostasis. *Kidney Int* 72: 140–142, 2007.

37. **O'Donnell JM, Fields AD, Sorokina N, Lewandowski ED.** The absence of endogenous lipid oxidation in early stage heart failure exposes limits in lipid storage and turnover. *J Mol Cell Cardiol* 44: 315–322, 2008.

38. **Orava J, Nuutila P, Lidell ME, Oikonen V, Noponen T, Viljanen T, Scheinin M, Taittonen M, Niemi T, Enerbäck S, Virtanen KA.** Different metabolic responses of human brown adipose tissue to activation by cold and insulin. *Cell Metab* 14: 272–279, 2011.

39. **Ouellet V, Labbé SM, Blondin DP, Phoenix S, Guérin B, Haman F, Turcotte EE, Richard D, Carpentier AC.** Brown adipose tissue oxidative metabolism contributes to energy expenditure during acute cold exposure in humans. *J Clin Invest* 122: 545–552, 2012.

40. **Park W, Kim BS, Lee JE, Huh JK, Kim BJ, Sung KC, Kang JH, Lee MH, Park JR, Rhee EJ, Oh KW, Lee WY, Park CY, Park SW, Kim SW.** Serum phosphate levels and the risk of cardiovascular disease and metabolic syndrome: a double-edged sword. *Diabetes Res Clin Pract* 83: 119–125, 2009.

41. **Saltiel AR, Kahn CR.** Insulin signalling and the regulation of glucose and lipid metabolism. *Nature* 414: 799–806, 2001.

42. **Schinagl DA, Span PN, Oyen WJ, Kaanders JH.** Can FDG PET predict radiation treatment outcome in head and neck cancer? Results of a prospective study. *Eur J Nucl Med Mol Imaging* 38: 1449–1458, 2011.

43. **Shaikh A, Berndt T, Kumar R.** Regulation of phosphate homeostasis by the phosphatonins and other novel mediators. *Pediatr Nephrol* 23: 1203–1210, 2008.

44. **Swanson HE.** Interrelations between thyroxin and adrenalin in the regulation of oxygen consumption in the albino rat. *Endocrinology* 59: 217–225, 1956.

45. **Takeda E, Yamamoto H, Nashiki K, Sato T, Arai H, Taketani Y.** Inorganic phosphate homeostasis and the role of dietary phosphorus. *J Cell Mol Med* 8: 191–200, 2004.

46. **Tanaka S, Yamamoto H, Nakahashi O, Kagawa T, Ishiguro M, Masuda M, Kozai M, Ikeda S, Taketani Y, Takeda E.** Dietary phosphate restriction induces hepatic lipid accumulation through dysregulation of cholesterol metabolism in mice. *Nutr Res* 33: 586–593, 2013.

47. **Vilardaga JP, Romero G, Friedman PA, Gardella TJ.** Molecular basis of parathyroid hormone receptor signaling and trafficking: a family B GPCR paradigm. *Cell Mol Life Sci* 68: 1–13, 2011.

48. **Wilson PW, D'Agostino RB, Parise H, Sullivan L, Meigs JB.** Metabolic syndrome as a precursor of cardiovascular disease and type 2 diabetes mellitus. *Circulation* 112: 3066–3072, 2005.

49. **Wojcik M, Dolezal-Oltarzewska K, Janus D, Drozdz D, Sztefko K, Starzyk JB.** FGF23 contributes to insulin sensitivity in obese adolescents - preliminary results. *Clin Endocrinol (Oxf)* 77: 537–540, 2012.

50. **Yamamoto KT, Robinson-Cohen C, de Oliveira MC, Kostina A, Nettleton JA, Ix JH, Nguyen H, Eng J, Lima JA, Siscovick DS, Weiss NS, Kestenbaum B.** Dietary phosphorus is associated with greater left ventricular mass. *Kidney Int* 83: 707–714, 2013.

51. **Yan L, Schoenmakers I, Zhou B, Jarjou LM, Smith E, Nigdikar S, Goldberg GR, Prentice A.** Ethnic differences in parathyroid hormone secretion and mineral metabolism in response to oral phosphate administration. *Bone* 45: 238–245, 2009.